



PII S0016-7037(00)00400-2

Interactions between metal oxides and species of nitrogen and iodine in bioturbated marine sediments

PIERRE ANSCHUTZ,^{1,*} BJØRN SUNDBY,² LUCIE LEFRANÇOIS,² GEORGE W. LUTHER III,³ and ALFONSO MUCCI⁴¹Département de Géologie et Océanographie, UMR 5805 EPOC, Université Bordeaux I, Talence 33405, France²Institut des Sciences de la Mer de Rimouski, Université du Québec à Rimouski, Rimouski, QC, Canada G5L 3A1³College of Marine Studies, University of Delaware, Lewes, DE 19958, USA⁴Earth & Planetary Sciences, McGill University, Montreal, QC, Canada H3A 2A7

(Received September 29, 1999; accepted in revised form March 23, 2000)

Abstract—By using a gold amalgam (Au/Hg) voltammetric microelectrode, we have measured simultaneously and with millimeter resolution the distributions of O₂, Mn(II), Fe(II), I(–I), and HS(–I) in bioturbated sediment cores from the Laurentian Trough. We also measured nitrate and ammonia in the pore water, total I and ascorbate- and HCl-extractable Fe and Mn in the solid-phase sediment, and fluxes of O₂, NO₃[–], and NH₄⁺ across the sediment–water interface. The concentrations of O₂ and Mn(II) were below their respective detection limits of 3 and 5 μM between 4 and 12 mm depth, but a sharp iodide maximum occurred at the depth where upward diffusing Mn(II) was being removed. We propose that the iodide peak is maintained through the reduction of IO₃[–] by Mn(II), reoxidation of I(–I) to IO₃[–] in the oxic zone above the peak and oxidation to I₂ below where it is ultimately trapped by reaction with organic matter. The iodide production rate is sufficient to account for the oxidation of all of the upward diffusing Mn(II) by IO₃[–].

Nitrate plus nitrite (ΣNO₃) decreased to a minimum within 10 mm of the sediment–water interface, in agreement with flux measurements which showed ΣNO₃ uptake by the sediment. Below the minimum, ΣNO₃ rebounded, and reached a maximum at 40- to 50-mm depth. This rebound is attributed to the anaerobic oxidation of ammonia by manganese oxides. Fe(II) was always first detected below the anoxic ΣNO₃ maximum, and was accompanied by colloidal or complexed Fe(III). A sharp upward-directed ammonia gradient was recorded near the sediment–water interface, but no ammonia was released during the first 48 h of the incubations. If the ammonia removal were due to coupled bacterial nitrification–denitrification, more than one half of the total measured oxygen uptake (6.7 to 7.3 mmol/m²/d) would be required, and more organic carbon would be oxidized by nitrate than by oxygen. This scenario is not supported by nitrate flux calculations. Alternatively, the oxidation of ammonia to N₂ by manganese oxides is a potential removal mechanism. It would require one quarter of the total oxygen flux.

The high-resolution profiles of redox species support the conceptualization of bioturbated sediments as a spatially and temporally changing mosaic of redox reactions. They show evidence for a multitude of reactions whose relative importance will vary over time, and for reaction pathways complementing those usually considered in diagenetic studies. Copyright © 2000 Elsevier Science Ltd

1. INTRODUCTION

The preferential use of the electron acceptor that yields the highest amount of free energy in the terminal step of the bacterially mediated oxidation of organic matter constitutes a long-standing paradigm in biogeochemistry (Froelich et al., 1979; Postma and Jakobsen, 1996). In undisturbed sediments, this paradigm is reflected in a well established depth zonation of redox reactions in which oxygen is reduced near the sediment–water interface, followed by the reduction of nitrate, manganese oxides, iron oxides, sulfate, and carbon dioxide. However, in sediments where the relative positions of reducing and oxidizing sediment components keep shifting because of bioturbation or other physical disturbances, the time sequence of redox reactions does not always translate to a similarly recognizable depth sequence. Nor does the concept of a vertical chemical zonation necessarily apply under such conditions. As

pointed out by Aller (1994a), such disturbed systems could be better conceptualized as a spatially and temporally changing mosaic of redox reactions.

Among the many possible redox reactions, those involving manganese and iron oxides can be particularly important because sediment particles located at or above the O₂ penetration depth commonly accumulate these oxides through the oxidative precipitation of dissolved manganese and iron. For example, the concentration of manganese dioxide in a volume of sediment of 0.9 porosity containing 1000 ppm Mn(IV) on a dry weight basis, common in coastal sediments (e.g., Sundby et al., 1993), would be 5 μmol/cm³, assuming a particle density of 2.65. This is more than one order of magnitude higher than typical dissolved oxygen concentrations in sediment pore water near the sediment–water interface. Near the sediment surface and in the vicinity of metal-rich particles biotransported into the anoxic sediment, reduced sediment components can encounter high concentrations of metal oxides with which they may react (Aller, 1994b). Examples of reactions involving metal oxides are the oxidation of ammonia to dinitrogen by manganese oxides in the presence of oxygen (Luther et al., 1997) and the oxidation of sulfide to sulfate and ammonia to

* Author to whom correspondence should be addressed (anschut@geocean.u-bordeaux.fr).

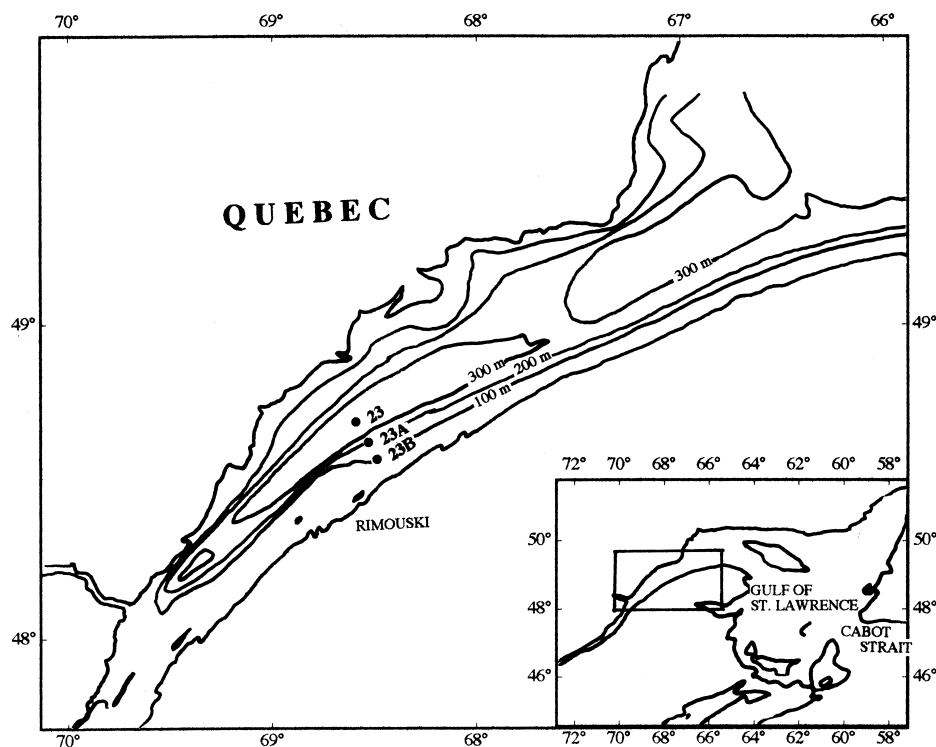


Fig. 1. Map of the study area showing the location of stations 23, 23A, and 23B.

nitrate by manganese oxides in the absence of oxygen (Aller and Rude, 1988; Hulth et al., 1999).

If we approximate bioturbation as a succession of mixing events, a bioturbated sediment can be thought of as an environment where the distributions of oxidants and reductants evolve towards, without necessarily achieving, a steady state before the next event disrupts the process. The extent to which mixing events affect the evolution towards a steady state depends on their frequency, for the higher the frequency, the less time is available for the concentration of a redox species to evolve towards the steady state before the next event occurs. It also depends on the concentration gradient across the interval being mixed, for the greater the concentration difference, the greater is the net flux. Vertical profiles of redox species are therefore likely to represent a transient state rather than a steady state. Here we report new measurements of electroactive species in continental margin sediments, made with a voltammetric microelectrode that can measure simultaneously and with millimeter resolution the concentrations of O_2 , $I(-I)$, $Mn(II)$, $Fe(II)$, and $HS(-I)$ in sediment pore water (Brendel and Luther, 1995; Luther et al., 1998). We use these data, in combination with solid-phase analyses and concurrent measurements of nitrate and ammonia profiles and fluxes to illustrate the dynamic nature of diagenesis in bioturbated sediments.

2. METHOD

2.1. Sample Collection

Undisturbed samples of fine-grained muddy sediments were collected by using a 20×30 cm box corer at 325 m (St. 23), 200 m (St. 23A), and 100 m depth (St. 23B) on a section across the sloping bottom

of the Laurentian Trough in the lower St. Lawrence Estuary off Rimouski in June 1997 (Fig. 1). The deepest station corresponds to St. 23 in Silverberg and Sundby (1990) and Sundby et al. (1981). The box cores were subsampled by pushing two 60 cm long, 10 cm diameter, Plexiglas tubes gently, to avoid compression, into each box core. The subcores, which were sealed with plastic caps, contained ~15 cm of overlying bottom water. The subcores were left in the box core until the ship reached the harbor (3 to 4 h) to take advantage of the thermal inertia of the mud and prevent warming. The six subcores were thus brought to the laboratory with minimal disturbance. The cores were kept refrigerated at the in situ temperature of 4°C for the duration of the experiment. One subcore from each station was used for flux measurements and a second core was used for sediment and pore-water analysis.

2.2. Pore-Water Profiling of O_2 , $Mn(II)$, $Fe(II)$, $I(-I)$, and $S(-II)$

The voltammetric gold amalgam microelectrodes used to measure these redox species were made by sealing a $100 \mu m$ gold wire in a glass capillary and plating mercury onto the polished exposed gold surface. The construction of the microelectrode is described in Brendel and Luther (1995) and Luther et al. (1998). A standard three-electrode voltammetric cell was used for all electrochemical measurements with the microelectrode as working electrode, a 0.5 mm diameter platinum wire as counter electrode, and a saturated calomel electrode (SCE) as reference electrode. The counter and reference electrodes were inserted into the surface of the core approximately 1 cm from the working electrode. An Analytical Instrument Systems, Inc. (AIS) model DLK-100 electrochemical analyzer was used for all measurements. The DLK-100 has a picoammeter detection system with full computer control which allows for excellent detection limits because both signal and noise can be distinguished at lower currents; it also allows the forward and reverse currents of a square wave voltammogram (which are opposite in sign) to be plotted along with the resultant current. The procedure for electrode calibration is described elsewhere (Brendel, 1995; Brendel and Luther, 1995).

Oxygen was determined with linear sweep voltammetry (LSV), scanning from -0.1 V to -1.7 V at a rate of 200 mV/s after 10 s equilibration at -0.1 V. I(-I), Mn(II), Fe(II), and HS(-I) were determined with square wave voltammetry (SWV). Before each scan, the electrode was conditioned for 30 s at -0.1 V to restore the electrode surface. This step removes any previously deposited reduced elements from the amalgam. The conditioning was followed by a scan from -0.1 V to -1.7 V in the square wave mode. In this mode the parameter values were: pulse height 15 mV, step increment 2 mV, frequency 100 Hz, and scan rate 200 mV/s. When HS(-I) was detected, we ran a second scan after a conditioning step at -0.85 V. Detection limits at the 99% confidence limit for O₂, Mn(II), Fe(II), I(-I), and HS(-I) are 3, 5, 15, <0.2 , and <0.2 μ M, respectively. Precision for replicates of all species at a given depth is typically 2 to 5%. I(-I) could not be determined below the depth where Fe(II) first appeared in the profile because the signal was masked by a broad peak, attributed to colloidal Fe(III) species (Taillefert et al., 2000), that occurred at the reduction potential for I(-I).

The microelectrode profiling was carried out at the in situ temperature immediately upon the arrival of the subcores in the laboratory. Each vertical profile consisted of ~ 100 measurements, taking ~ 2 min each. Core 23B was analyzed first, followed immediately by core 23 and core 23A. Thus, all microelectrode measurements were completed within 15 h of sampling.

A recent in situ deployment comparing oxygen measurement with Clark-type and voltammetric micro-electrodes showed excellent agreement (Luther et al., 1999). Likewise, agreement within 5% was obtained between direct pore-water measurements of Fe(II) and measurement of pore water recovered by slicing and centrifuging sediment samples (Brendel and Luther, 1995).

2.3. Pore-Water Extraction and Porosity Determination

As soon as the micro-profiling was completed, the cores from St. 23 and St. 23B were sectioned in 0.5, 1, or 2 cm vertical intervals in a glove bag under a stream of nitrogen. An aliquot of the wet sediment of known volume and weight was freeze-dried and the weight loss was used to calculate porosity (Bernier, 1980). The dried solid was homogenized and kept for solid-phase analysis. The remainder of the sediment was transferred to resealable polyethylene tubes and centrifuged 20 min under nitrogen at 3000 rpm to extract the pore water. The pore-water samples were filtered (0.4 μ m) and an aliquot was immediately analyzed for ammonia. The remaining sample was frozen and processed within a few days for nitrate + nitrite (Σ NO₃). The cores from St. 23 and 23B were processed rapidly, but the processing of the core from St. 23A was postponed by two days because of time constraints. Although the core was kept at the in situ temperature during this time, it is possible that the delay led to changes in the distributions of ammonia and nitrate. This is taken into consideration in the discussion of the data.

2.4. Solid-phase Analysis

The freeze-dried solid from the porosity determination was homogenized in preparation for analysis. The water content and the salinity were used to correct the analyses for the presence of sea salt. Samples from the top 10 cm of the cores and a sample from the bottom of each core were subjected to two different extraction techniques. The most reactive iron oxide fraction (amorphous oxides) was extracted with an ascorbate reagent (Anschutz et al., 1998; Ferdelman, 1988; Kostka and Luther, 1994). This reagent consisted of a deaerated solution of 10 g of sodium citrate and 10 g of sodium bicarbonate in 200 mL of deionized water to which 4 g of ascorbic acid was slowly added to a final pH of 8. About 100 mg of dry sediment was extracted at room temperature with 13 mL of this reagent while shaking continuously for 24 h. A second extraction on a separate 200 mg aliquot was carried out with 35 mL of 1 N HCl for 6 h to determine acid soluble Mn and Fe. The centrifuged solutions were then diluted in 1 N HCl and analyzed.

Unlike Fe, similar amounts of Mn were extracted from the freeze-dried solids by the two reagents. The ascorbate reagent extracts selectively amorphous iron and manganese oxides and associated elements (Kostka and Luther, 1994). The reactive phases extracted by 1 N HCl represented the operationally defined fraction that comprises amor-

phous and crystalline Fe and Mn oxides, carbonates and hydrous aluminum silicates (Huerta-Diaz and Morse, 1990; 1992) but may not include the oxidation products of Fe monosulfides (goethite and hematite; Raiswell et al., 1994). Consequently, Fe_{ASC} is expected to be smaller than Fe_{HCl}. There are flaws inherent in any extraction procedure but even critics of these techniques concede that they are useful tools when used and interpreted with caution. We are aware that the solid-phase speciation of metals may change upon oxidation and freeze-drying of the sediments (Rapin et al., 1986). The most significant change is the oxidation of acid volatile sulfides (AVS) to oxides that are not readily extracted by the 1 N HCl reagent (Raiswell et al., 1994).

Total iodine was determined by X-ray fluorescence (XRF) using a Philips model PW2400 spectrometer equipped with a rhodium 60 kV end-window X-ray tube. The analysis was carried out on 40-mm diameter pressed pellets prepared by mixing the freeze-dried sediment with Hoechst Wax C Micropowder (5:1). The instrument was calibrated by using IS-40 Certified International Reference Materials. The detection limit, based on three times the background sigma value, was 1 mg/kg.

2.5. Flux Measurements

Immediately upon arrival in the laboratory, subcores from each of the three stations were incubated at 4°C in the dark to measure the fluxes of oxygen, nitrate, and ammonia across the sediment-water interface, by using the procedures described in Hulth et al. (1994). A Plexiglas lid, equipped with a magnetic stirring bar rotating at 30 rpm and Teflon valves for sampling, capped the core barrel containing the sediment and ~ 12 cm (1 L) of supernatant water. Care was taken to avoid trapping air bubbles under the lid. Water samples were collected from each core eleven times during the 110 h of incubation. A 50 mL sample was drawn into a glass syringe for oxygen analysis by the Winkler method and another 15 mL was collected with a plastic syringe and immediately filtered through a 0.45 μ m filter for ammonia and nitrate measurements. As the samples were drawn, they were replaced by an equal volume of St. 23B bottom water of known oxygen, nitrate, and ammonia concentrations. The measured concentrations in the samples were corrected for the amount added with the replacement water. Within the range of concentrations measured, the precision (one standard deviation) of the oxygen, nitrate and ammonia analyses was approximately 5 μ M, 1 μ M, and 1 μ M, respectively. The error after correcting for the addition of replacement water is estimated to be twice the analytical precision.

2.6. Analytical Procedures

Fe and Mn extracted from the sediment were measured by flame-atomic absorption spectroscopy, using aqueous standards. Ammonia was measured by using the flow injection method described by Hall and Aller (1992), and nitrate plus nitrite (Σ NO₃) were measured by the flow injection method of Anderson (1979). The analytical precision of these methods is better than 5%.

3. RESULT

3.1. Sediment Composition

The sediment cores consisted of fine-grained olive green muds with a thin (<1 cm) brown surface layer. The sediments in the Laurentian Trough are bioturbated (Silverberg et al., 1986), and we found one or two living polychaete worms in each core. The porosity at St. 23 decreased exponentially from 88% in the surface layer to 75% at 35 cm. The porosity profiles at St. 23A and St. 23B were similar to St. 23, but at corresponding depths the porosities were shifted towards lower values by 2 and 5%, respectively.

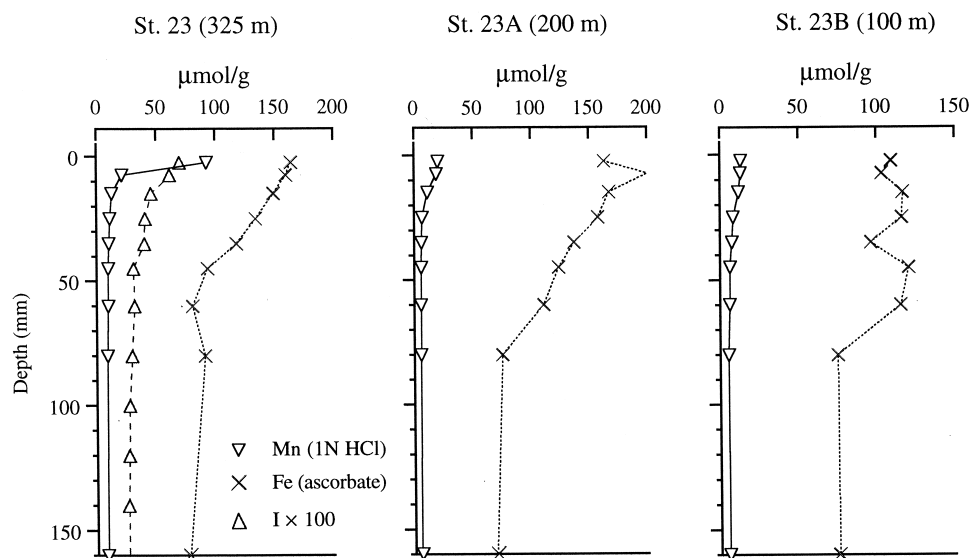


Fig. 2. Vertical distributions of reactive particulate Mn and Fe at stations 23, 23A, and 23B ($\mu\text{mol/g}$ dry wt.) and total I at station 23 ($100 \times \mu\text{mol/g}$ dry wt.).

3.1.1. Manganese

Each of the three cores was enriched in acid soluble manganese in the surface layer (Fig. 2). The enrichment is due to the presence of authigenic manganese oxides (Sundby et al., 1981). The manganese inventory, integrated over the top 4 cm, was 10.1, 20.1, and 10.7 $\mu\text{mol/cm}^2$ for stations 23, 23A, and 23B, respectively. However, in the 0 to 5 mm surface layer, the manganese concentration was highest at the deepest station (St. 23; 92.8 $\mu\text{mol/g}$) and lowest at the shallowest station (St. 23B; 13.4 $\mu\text{mol/g}$). Below 4 cm depth, the concentration of acid soluble Mn was approximately constant at 5 to 10 $\mu\text{mol/g}$. The manganese distribution at St. 23 was nearly identical to that reported by Sundby et al. (1981) except that it was lower by $\sim 10 \mu\text{mol/g}$ at each depth, which we ascribe to procedural differences, i.e., total vs. acid soluble manganese.

3.1.2. Iron

Ascorbate-extractable iron concentrations in the top 1 cm were 100 to 200 $\mu\text{mol/g}$ with the lowest values at the shallowest station. Extractable iron decreased with depth and reached 50 to 60 $\mu\text{mol/g}$ towards the bottom of the cores. The vertical distribution of HCl-extractable Fe was similar but the absolute amounts extracted were 200 to 300 $\mu\text{mol/g}$ higher (Fig. 2).

3.1.3. Iodine

Total iodine was measured in one core (St. 23). Iodine decreased exponentially from 0.71 $\mu\text{mol/g}$ in the top 5 mm and reached background values of $0.24 \pm 0.04 \mu\text{mol/g}$ at ~ 10 cm depth (Fig. 2).

3.2. Pore-Water Composition and Solute Fluxes

3.2.1. Oxygen

In all three cores, the oxygen concentration decreased sharply across the sediment-water interface and became unde-

tectable at 3 to 4 mm depth (Fig. 3). Oxygen penetration depths of 2 to 10 mm at St. 23, measured with a Clark-type polarographic microelectrode, were reported by Silverberg et al. (1987). During the core incubations, the samples withdrawn were replaced with water of high and known oxygen content in an attempt to keep the oxygen concentration in the overlying water from falling. Despite this precaution, the oxygen concentration in the overlying water kept decreasing and was typically reduced to 25% of the initial concentration towards the end of the 110 h incubations. The decreasing oxygen concentration will ultimately affect the flux into the sediment (e.g., Hall et al., 1989), but during the first 40 h of the incubation, oxygen remained above 70% of the initial concentration and the oxygen flux was approximately constant (r^2 better than 0.964). The oxygen uptake rate thus estimated was similar for the three cores with values ranging from 6.7 to 7.3 $\text{mmol/m}^2/\text{d}$ (Fig. 4, Table 1). By using the concentration gradient between 0 and 1 mm depth and measured porosity, and assuming oxygen transport by molecular diffusion, we estimate oxygen fluxes into the sediment of 2 to 5 $\text{mmol/m}^2/\text{d}$. The highest flux was at the shallowest station. These estimates are lower than those measured in incubated cores. Bioturbation or roughness of the surface may be responsible for the difference.

3.2.2. Iodide

In each of the three cores, the iodide concentration increased across the sediment-water interface to maximum concentrations of 6 to 7 μM at ~ 13 mm depth (Fig. 3). This is one order of magnitude higher than the total iodine content of seawater. In each core, the depth of the iodide maximum coincided with the depth where Mn(II) first became detectable (Fig. 5). Below the maximum, iodide decreased progressively, but iodide could not be measured with the microelectrode below the depth where Fe(II) was first detected (see Sections 2.2, 4.2.1, and 4.4).

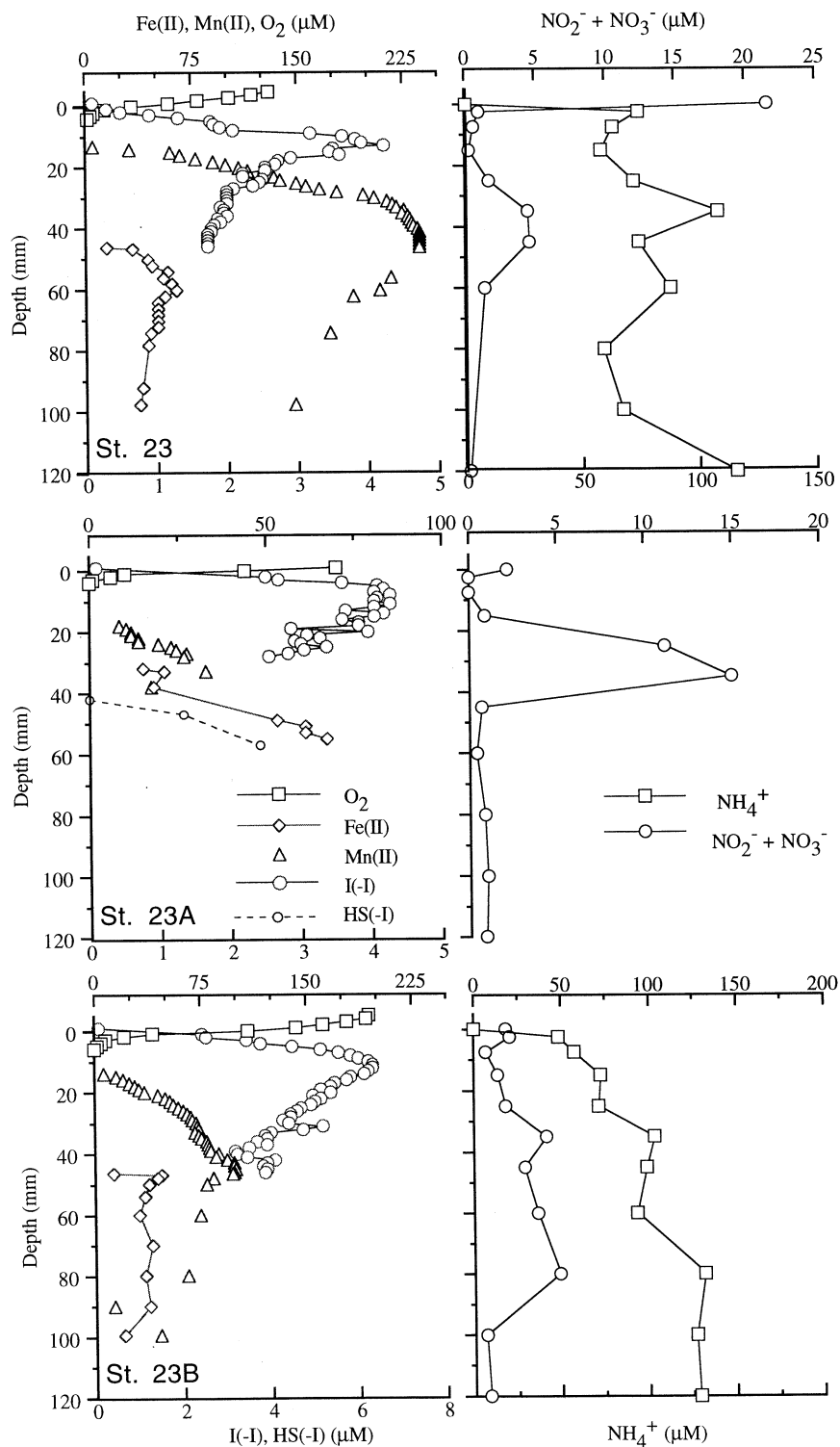


Fig. 3. Left: Vertical distributions of dissolved O₂, I(-I), Mn(II), Fe(II), and HS(-I) in sediment pore waters at stations 23, 23A, and 23B, in μM. The profiles were acquired with a solid-state gold/mercury amalgam microelectrode (Brendel and Luther, 1995). The detection limits for O₂, I(-I), Mn(II), Fe(II), and HS(-I) were 3 μM, 5 μM, 15 μM, <0.2 μM, and <0.2 μM, respectively. The iodide concentration in St Lawrence Estuary bottom water is <0.1 μM (Takayanagi and Cossa, 1985). Right: Vertical distributions of dissolved ammonia and ΣNO₃⁻ (μM) in sediment porewater at stations 23, 23A, and 23B. These measurements were made on porewater samples extracted from the cores used for microelectrode profiling. Note that the concentration scale varies among the cores.

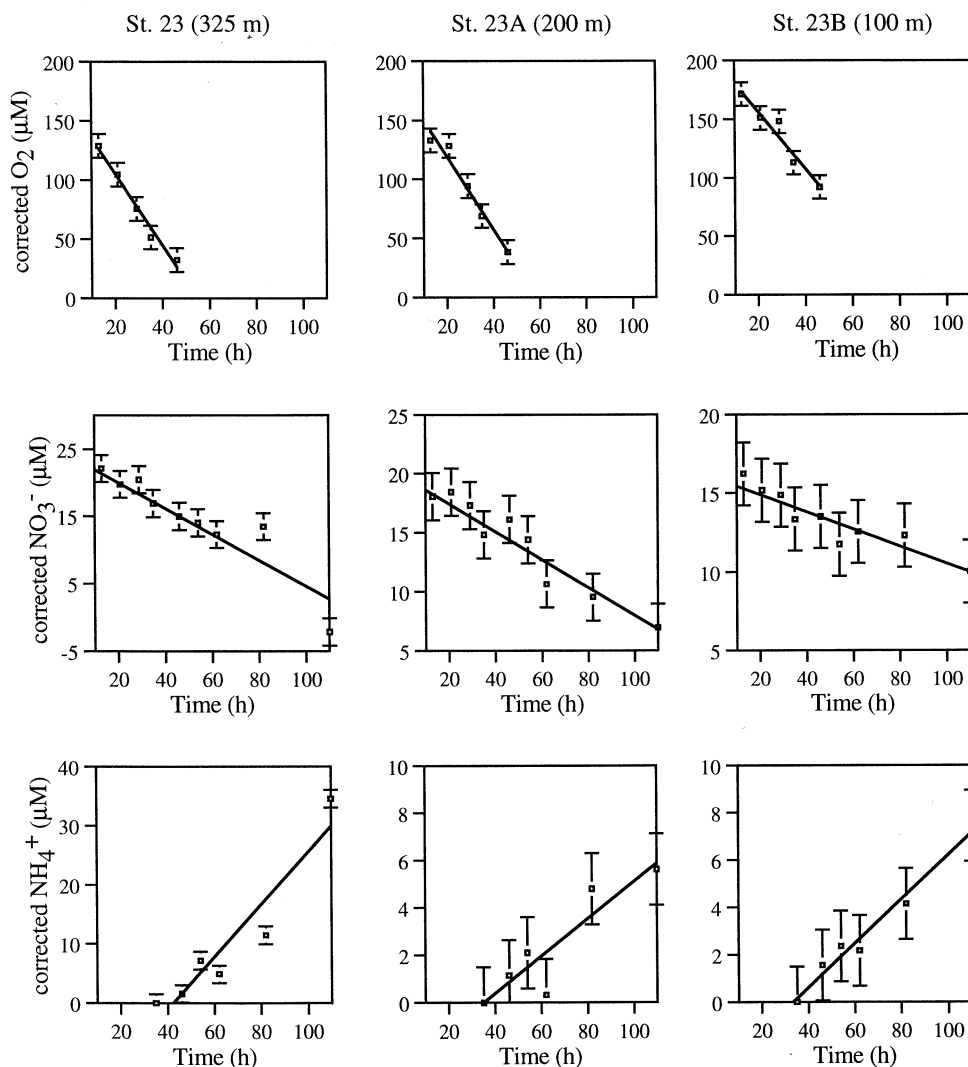


Fig. 4. Temporal variation of dissolved oxygen (top), ΣNO_3^- (middle), and ammonia (bottom) in the overlying water during core incubations. Station 23 (left), 23A (middle), and 23B (right). The values have been corrected for the amount of each solute contained in the replacement water added when sampling. The benthic fluxes were calculated from the linear regression lines. Note that there was no detectable release of ammonia from any of the cores during the first 48 h of the incubation.

3.2.3. ΣNO_3 (nitrate + nitrite)

The bottom water ΣNO_3 concentration at the three stations, measured in the overlying water recovered with the box cores, was 16.3, 18.9, and 21.9 μM , respectively, for St. 23B, 23A, and 23. These values agree with the reported depth distribution of nitrate in the Laurentian Trough (Yeats, 1988). The vertical resolution of ΣNO_3 and ammonium, which were measured on squeezed samples, is not as good as for the pore-water constituents measured with the microelectrode. Nevertheless, the vertical profiles of nitrate displayed a clear minimum within 10 mm of the sediment–water interface and, surprisingly, a broad maximum below this, in the 40 to 80 mm depth range (Fig. 3). In one core (St. 23B) the ΣNO_3 concentration reached 48 μM at 80 mm depth. This is much higher than in the overlying bottom water, which indicates that the high nitrate concentra-

tion is not due to the infiltration of bottom water through animal burrows. The weak concentration gradient across the sediment–water interface in core 23A is likely an artifact due to the 3-day delay between core recovery and subsampling of this core. During this time the ΣNO_3 concentration in the supernatant water had decreased from the initial 18.9 μM to 2 μM because of ΣNO_3 consumption within the sediment, as observed during the incubations. In the two other cores, which were processed soon after recovery, the ΣNO_3 concentration in the supernatant had only decreased by 3 μM . The direction of the ΣNO_3 concentration gradient across the sediment–water interface, which would drive ΣNO_3 into the sediment, agrees with the incubations. These gave nitrate fluxes of $-0.46 \text{ mmol/m}^2/\text{d}$ for St. 23, $-0.25 \text{ mmol/m}^2/\text{d}$ for St. 23A, and $-0.16 \text{ mmol/m}^2/\text{d}$ for St. 23B (Fig. 4, Table 1).

Table 1. Incubation results: fluxes of oxygen, nitrate, and ammonia at the sediment–water interface.

	Oxygen uptake rate (mmol/m ⁻² /d ⁻¹)	Nitrate uptake rate (mmol/m ⁻² /d ⁻¹)	Ammonia release rate (mmol/m ⁻² /d ⁻¹)	
			0–40 h	After 40 h
St. 23	–7.3	–0.46	0	1.05
St. 23A	–6.7	–0.25	0	0.17
St. 23B	–7.3	–0.16	0	0.28

3.2.4. Ammonia

The ammonia concentration in the water overlying the cores at the time of their collection was below our detection limit (1 μM). Between the overlying water and the first pore–water sample (the 0 to 5 mm interval), the ammonia concentration increased by 50 μM at St. 23B and by 70 μM at St. 23. Below this depth, the ammonia concentration increased gradually and reached values as high as 230 μM and 380 μM , respectively, near the bottom of cores 23B and 23 (data not shown on the figures). We are not reporting the ammonia profile for St. 23A because of the delay in processing this core. In spite of the sharp increase in ammonia concentration across the sediment–water interface, ammonia was not detected in the overlying water during the initial 48 h of the incubations. During the following 64 h, ammonia was released from the sediment at constant rates of 1.05 mmol/m²/d (St. 23), 0.17 mmol/m²/d (St. 23A), and 0.28 mmol/m²/d (St. 23B; Fig. 4, Table 1).

3.2.5. Dissolved manganese

Mn(II) was first detected at 13 mm depth in cores from St. 23 and St. 23B, nearly 10 mm deeper than the depth where oxygen became non-detectable (Fig. 3). We cannot exclude that some Mn(II) was present above 13 mm at concentrations below our detection limit (5 μM), nor that some dissolved oxygen penetrated below 4 mm. However, the slopes of the profiles (Fig. 3) show that the major process consuming the upward diffusing Mn(II) occurred at, or just below, 12 mm depth and that the

major sink for oxygen was above 4 mm depth. Similar observations, i.e., the presence of a depth interval in which neither O₂ nor Mn(II) is detectable, have been made in previous studies (Luther et al., 1998; Luther et al., 1997). In each of the three cores, the depth where manganese was first detected coincided with the depth of the iodide maximum. As the concentration of Mn(II) continued to increase with depth, the iodide concentration decreased. The Mn(II) maximum occurred at approximately the same depth as the subsurface nitrate maximum.

Below the dissolved manganese maximum, Mn(II) decreased progressively with depth. Dissolved manganese is most likely precipitated as a mixed calcium–manganese carbonate (Middelburg et al., 1987; Mucci, submitted) as the pore waters become supersaturated with respect to both calcite and rhodochrosite after the production of carbonate alkalinity via sulfate reduction. Measurements of sulfate reduction rates (SRR) from a core recovered at this site and a depth of 335 m showed that SRR increased rapidly below ~ 5 cm and that titration alkalinities reached more than 6 meq/kg by 30 cm depth (Edenborn et al., 1987). Alternatively, the pore–water manganese may be scavenged by adsorption onto acid volatile sulfides (AVS) (Arakaki and Morse, 1993) the concentration of which increases below 5 cm at this site (from ~ 3.5 to 30 mmol/g at 10 cm; Gagnon et al., 1995). Unfortunately, it has been impossible to confirm the fate of the pore–water manganese. Because of low abundance and high reactivity, the relevant solid phases cannot be readily isolated.

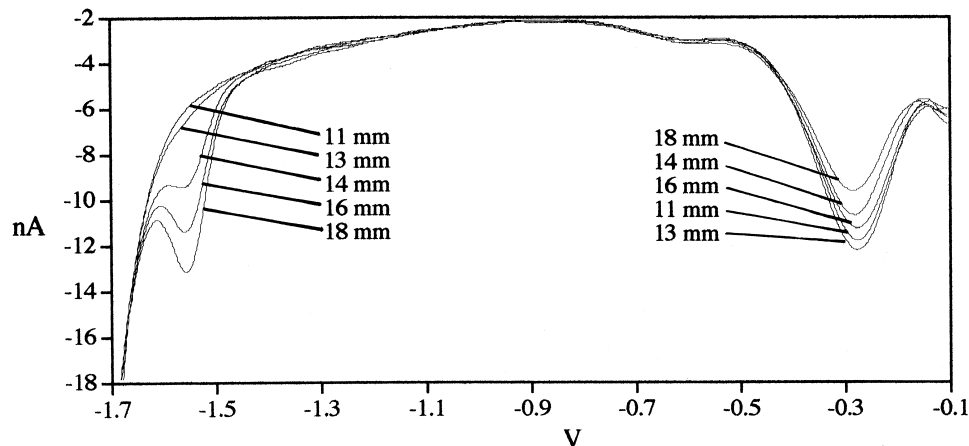


Fig. 5. Overlay of five square wave voltammograms obtained with a gold/mercury amalgam microelectrode at successive depth (11, 13, 14, 16, and 18 mm) below the sediment–water interface at St. 23. Oxidation of I(–I) and reduction of Mn(II) at the electrode surface took place at -0.3 V and -1.49 V, respectively. The peak height is proportional to the concentration. The maximum concentration of I(–I) concurred with the first value of Mn(II) above the detection limit.

3.2.6. Dissolved iron

Fe(II), measured as a peak at -1.43 V, was first observed at 35 to 46 mm depth, depending on the core. The concentration of Fe(II) when it first occurred, was well above the detection limit for Fe(II) ($15 \mu\text{M}$), indicative of a sharp concentration gradient and suggesting the presence in this layer of the major sink of upward diffusing Fe(II). The depth of the first Fe(II) occurrence corresponds to the Mn(II) and nitrate maxima. The appearance of Fe(II) was accompanied by a broad peak at -0.4 V in the voltammogram, consistent with the presence of colloidal or dissolved Fe(III) complexes (Brendel and Luther, 1995; Huettel et al., 1998). Some of the Fe(II) measured at -1.43 V probably arose from the reduction of colloidal Fe(III) at the electrode, and the values of Fe(II) given in the pore-water profiles must therefore be considered as maximal. However, there was no relationship between the height of the -0.4 V and the -1.43 V peaks in the voltammograms, indicating that both Fe(II) and Fe(III) were present in the pore water.

3.2.7. Dissolved sulfide

No dissolved sulfide could be detected in cores 23 and 23B over the depth interval examined with the microelectrode (0 to 100 mm) although the smell of sulfide was noted deeper in the cores. In core St. 23A, sulfide was detected below 45 mm depth.

4. DISCUSSION

4.1. Non-steady State Diagenesis

By definition, the distribution of a sediment property is at steady-state if, at a fixed depth relative to the sediment–water interface, the property remains constant (Berner, 1980). The steady state is a useful idealization, but real sediment properties vary on various spatial and temporal scales. According to the definition, the distribution of solid-phase manganese in these sediments is at steady state over a time scale of years because the distributions we observe (St. 23) are virtually identical to observations made nearly 20 yr previously (Sundby et al., 1981) in spite of a sedimentation rate of ~ 2 mm per year (Silverberg et al., 1986). However, the shape of the dissolved Mn(II) profile shows that the manganese system is not at steady state. If it were, we should have observed a solid-phase manganese peak near the depth where dissolved Mn is being removed, i.e., at 13 mm depth (e.g., Burdige and Gieskes, 1983). Strictly speaking, the solid-phase and pore-water profiles may not be comparable because they were sampled on different spatial scales, i.e., a 0.5 to 2 cm long, 10 cm diameter sediment cylinder for the solid phase vs. a small volume near the surface of the $100 \mu\text{m}$ diameter electrode surface for Mn(II); yet, a similar offset between solid-phase and pore-water profiles was observed when both phases were sampled on the same spatial scale (Gobeil et al., 1997). Given the non-steady state distribution of manganese species, we can assume that the distributions of other redox species also are transient. The profiles, and the fluxes that can be deduced from them, are thus only representative of the time when the cores were collected and do not represent an average or a steady state. These profiles provide an instantaneous picture of the many

reactions that take place in a sediment rather than an integrated view of dominant diagenetic reactions.

4.2. The Role of Manganese in Non-steady State Diagenesis of Iodine and Nitrogen Species

Because of the ease with which it moves between the reduced and oxidized states within the Eh–pH range commonly encountered in marine sediments, manganese can participate both as oxidant (electron acceptor) and reductant (electron donor) in diagenetic reactions. Manganese oxide can serve as terminal electron acceptor in the bacterially mediated oxidation of organic matter (e.g., Froelich et al., 1979), as oxidant of sulfides (Aller and Rude, 1988), and as oxidant of ammonia producing either N_2 (Luther et al., 1997) or nitrate (Hulth et al., 1999). Other than the reaction with oxygen (Stumm and Morgan, 1996), redox reactions involving Mn(II) oxidation are not well documented, but it has been proposed that Mn(II) may reduce nitrate to N_2 (Aller, 1990; Luther et al., 1997).

4.2.1. The oxidation of Mn(II) near the sediment–water interface

Conventionally, we would presume that the peak in solid-phase manganese located in the 0 to 5 mm surface layer is created by the oxidation of soluble Mn(II) to insoluble Mn(III/IV) oxides by oxygen, which is present in this layer. At the time our cores were collected, however, this scenario did not seem operative because Mn(II) was not detected above 13 mm depth. This suggests that manganese was being precipitated well below the depth of the solid-phase manganese maximum. Furthermore, because O_2 was undetectable below 4 mm, the data imply that O_2 was not a major oxidant of Mn(II).

There are numerous reports of a layer of substantial thickness, both in sediments and in the water column, in which both O_2 and Mn(II) are below their respective detection limits, and it has been proposed that Mn(II) can be oxidized by NO_3^- (Aller, 1990; Schulz et al., 1994; Murray et al., 1995; Sørensen et al., 1987; Luther et al., 1997; 1998; Hulth et al., 1999). Consistent with this hypothesis, the nitrate distributions in our cores go through a minimum located approximately at the depth where Mn(II) is disappearing.

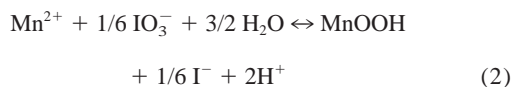
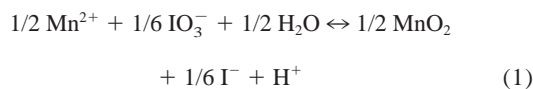
However, nitrate is not the only reactant other than oxygen that may oxidize Mn(II). An alternate and perhaps competitive oxidant is iodate, which occurs dissolved in seawater and adsorbed on sediment particles near the sediment–water interface (Ullman and Aller, 1985). The oxidation of Mn(II) by iodate (IO_3^-) is thermodynamically favorable and the reaction yields free energy equivalent to the corresponding reaction between Mn(II) and nitrate (Luther et al., 1997). Ullman and Aller (1985) proposed that a redox cycle for iodine exists near the sediment–water interface whereby iodide released during the decomposition of organic matter diffuses to the sediment–water interface where it is oxidized microbially to iodate, which is then adsorbed onto metal oxides; upon burial and reduction of the carrying phases, the adsorbed iodate is released to solution and may participate in redox reactions. Keeping in mind the transient nature of pore-water profiles in bioturbated sediments, the iodide and total iodine distributions we observe are consistent with this mechanism. The sediment surface layer

is enriched in total iodine by a factor of three over the subsurface sediment. Although the speciation was not determined, the solid-phase iodine is probably a mixture of organic-I and iodate adsorbed onto iron(oxy)hydroxides. The pore-water iodide distribution displays a sharp and well defined subsurface maximum with concentrations (4.2 μM at St. 23 and 23A and 6.3 μM at St. 23B) one order of magnitude higher than the total abundance of iodine in seawater (0.45 μM , mostly as iodate; Luther et al., 1988). However, further work on the distribution of the various iodine species both in the solid phase and in the pore water will be needed to confirm this mechanism.

A remarkable aspect of the data set is that, at each of the three sites, the iodide maximum coincided with the depth where the upward diffusing Mn(II) became undetectable. This suggests a coupling of the iodine and manganese cycles, i.e., that upward diffusing Mn(II) is oxidized by an iodine species, most likely iodate. In order for iodate reduction to be quantitatively important in a reaction with Mn(II), the production rate of iodide should be stoichiometrically of the same order of magnitude as the upward flux of Mn(II). We can estimate a rate of iodide production by assuming that it is balanced by the combined upward and downward fluxes of iodide from the iodide maximum. The fluxes can be calculated, assuming transport by molecular diffusion, from the two concentration gradients according to Fick's first law: $J = -\phi D_s dC/dX$, where J is flux, ϕ is the porosity, dC/dX is the concentration gradient, and D_s is the bulk sediment diffusion coefficient corrected for tortuosity, i.e., $D_s = D_o/\theta^2$ where θ is the tortuosity and D_o is the diffusion coefficient in water (Berner, 1980). D_o values were obtained from Li and Gregory (1974) and the value of θ^2 is assumed to equal $1 - \ln(\phi^2)$ (Boudreau, 1996). For the data set of St. 23, the upward directed iodide gradient between 13 mm and the sediment-water interface is 3.23 nmol/cm⁴. The mean porosity over that interval is 0.86 and D_s is 9.31 $\cdot 10^{-6}$ cm²/s, giving an upward flux of 0.026 pmol/cm²/s. The downward concentration gradient is 2.4 nmol/cm⁴, and with a porosity of 0.85 the downward flux of iodide is estimated at 0.019 pmol/cm²/s. The combined flux of iodide away from the peak is thus 0.045 pmol/cm²/s, or 0.39 mmol/m²/d. This is nearly one tenth of the oxygen flux into the sediment. These calculations assume steady state and the results only apply to the time when the cores were collected.

Before comparing the iodide production rate with the manganese flux we need to consider the possibility that the iodide production is a result of the remineralization of organic matter, the ultimate source of iodine, which is known to release dissolved iodide to the pore water (Kennedy and Elderfield, 1987; Ullman and Aller, 1983, 1985; Ullman and Sandstrom, 1987). The average molar I/C_{org} ratio is $\sim 4 \times 10^{-4}$ in settling particulate matter (Shimmield and Pedersen, 1990). If we assume that iodide is released in this proportion and at the same rate as the remineralization of organic carbon, and further that this rate is approximated by the oxygen uptake rate, we obtain a release rate of iodide of approximately 0.0028 mmol/m²/d. This is more than two orders of magnitude less than the iodide production rate we estimated above, and, therefore, an unlikely source for the observed subsurface iodide maximum. We propose that the latter originates mostly from the reduction of iodate by Mn(II). The possible reactions involved depend on whether the oxidation product is MnO₂ or MnOOH, but both

reactions are thermodynamically favorable (Luther et al., 1997).



We can now compare the iodide production rate with the upward flux of Mn(II). At St. 23, the Mn(II) gradient, which is approximately linear across the 13 to 31 mm depth interval, is estimated as 118 nmol/cm⁴. The average porosity is 0.83 and D_s is 2.77 $\times 10^{-6}$ cm²/s, which gives a Mn(II) flux of 0.271 pmol/cm²/s. This is six times the iodide production rate. Considering the stoichiometry of Reactions 1 and 2, each mole of IO₃⁻ oxidizes 3 or 6 mol of Mn(II), depending on the end-product. Assuming that the production rate of iodide can be equated with the reduction rate of iodate, the reduction of iodate may thus account for 50 to 100% of the oxidation of the upward diffusing manganese. At St. 23A and 23B the respective concentration gradients give higher values for the iodide production rate and lower values for the Mn(II) flux. At these stations the estimated reduction rate of iodate is more than sufficient to account for the oxidation of all the Mn(II), irrespective of the oxidation end-product.

The above conclusions apply only to the conditions at the time of sampling. Because of the location of the solid-phase manganese near the oxic sediment-water interface, oxygen reduction is probably the ultimate process that oxidizes and precipitates dissolved manganese. The data do suggest, however, that reactions between the iodine and manganese species can be important during the diagenesis of marine sediments. Moreover, they show that the relative importance of the many possible diagenetic reactions involving manganese may be changing over time, re-enforcing the view of diagenesis as a temporally and spatially variable web of redox reactions.

4.2.2. The fate of downward-diffusing iodide

To maintain the sharp pore-water iodide maximum observed in these cores, iodide must be removed both above and below the peak. Oxidation to iodate by oxygen may explain the removal above (e.g., Kennedy and Elderfield, 1987) but not below the maximum. The direct loss of iodide from anaerobic pore waters has not been reported previously. A series of experiments conducted by François (1987) showed that I(-I) was not sequestered by the solid sediment whereas the oxidized iodine species (IO₃⁻, I₂, and HIO) were. The removal of iodide that we observe in our cores is, therefore, likely due to the production of an oxidized iodine species, which in turn reacts with the solid phase. An examination of the profiles shows that the downward-diffusing iodide encounters upward diffusing nitrate. One possibility is therefore that iodide is oxidized by nitrate in a reaction that yields N₂ and I₂. This reaction, which is thermodynamically favorable at all pH encountered in marine sediments (Fig. 6), is intriguing not only because it would promote denitrification, but also because I₂ is highly reactive and could react further with organic matter to produce iodine-

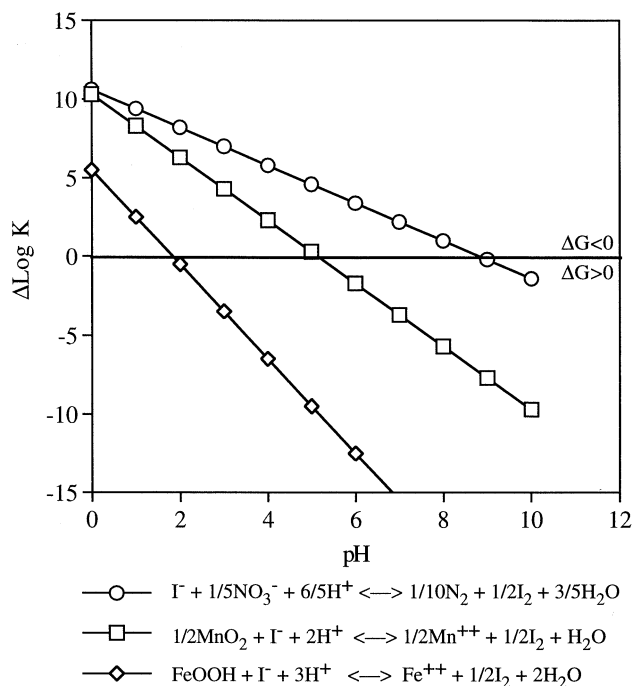


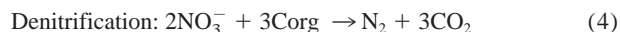
Fig. 6. $\Delta \log K$ vs. pH plots for selected reactions oxidizing I(-I) to I_2 . $\Delta \log K$ is the total free energy at a given pH. Positive $\Delta \log K$ indicates a thermodynamically favorable reaction.

ated organic molecules (Truesdale, 1982; François, 1987) which then would be buried. In a sense, this reaction would close the cycle whereby the iodine that is delivered to the sediment in association with organic matter, is released to the pore water via hydrolysis, oxidized to a more reactive species, and finally recombined with organic matter and buried.

4.2.3. The reduction of oxidized manganese near the sediment-water interface

It has recently been proposed that, in the presence of oxygen, manganese oxide may oxidize ammonia to dinitrogen in addition to serving as a terminal electron acceptor in the bacterial oxidation of organic matter (Luther et al., 1997). Furthermore, it has been shown that manganese oxide may oxidize ammonia to nitrate anaerobically (Hulth et al., 1999). The first, and maybe also the second, of these reactions could explain our observation that no ammonia could be seen to escape from the sediment to the overlying water during the first 48 h of the core incubations in spite of the sharp ammonia gradient near the sediment-water interface. The second of these reactions is possibly related to the presence of NO_3^- in the anoxic sediment.

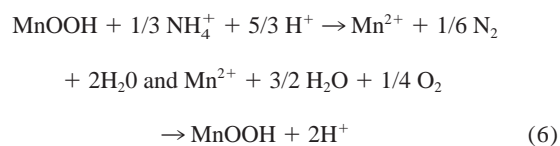
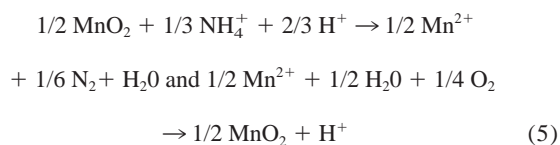
The processes that intercept the upward ammonia flux are quantitatively important, for if we assume a linear concentration gradient between the middle of the first sampling interval (0 to 5 mm) and the sediment surface, and transport by molecular diffusion, the "missing" ammonia flux is 2.05 and 1.20 $mmol/m^2/d$ at St. 23 and St. 23B, respectively. If the missing ammonia flux is consumed by coupled bacterial nitrification-denitrification, then according to:



two moles of O_2 are consumed for each mole of NH_4^+ . Hence, converting the "missing" ammonia to nitrate would require a supply of 4.1 $mmol/m^2/d$ of oxygen at St. 23, or more than half of the total sediment oxygen consumption.

The above scenario would require that nitrate be consumed faster than it is produced, because no build-up of nitrate was noted below the sediment-water interface. In fact, we measured a flux of nitrate from the overlying water into the sediment, thus denitrification at, for example St. 23, must proceed at a rate in excess of $(2.05 + 0.46)$ $mmol N/m^2/d$. This would also imply that more carbon is oxidized by nitrate than by oxygen. The presence of oxygen is usually thought to inhibit denitrification, which requires that nitrate be transported below the oxygenated sediment layer, i.e., below ~ 5 mm depth, to be denitrified. By using Fick's law of diffusion again, and assuming that denitrification takes place at 5 mm depth, we can calculate the downward nitrate flux to the top of the anaerobic layer. The concentration gradient is taken to be linear between the sediment-water interface (20 μM) and 5 mm depth (0 μM), the porosity is 0.86, and the diffusion coefficient is 5.1×10^{-6} cm^2/s . The diffusive flux to 5 mm depth is estimated at 0.19 $mmol/m^2/d$, or more than one order of magnitude less than the rate of nitrate consumption required by bacterial denitrification. In other words, this estimate represents the flux of nitrate from the aerobic zone (nitrification plus byproduct of ammonium oxidation) to the anaerobic zone. It suggests that aerobic nitrification coupled to anaerobic denitrification cannot alone account for the removal of ammonia diffusing to the interface.

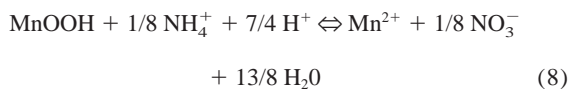
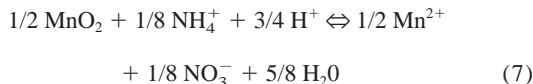
There exist several alternatives that may explain the data, none of which can be confirmed or ruled out at this time. One is that the denitrification process is carried out by aerobic bacteria, which would eliminate the need for transporting nitrate from the aerobic to the anaerobic zone of the sediment (Frette et al., 1997; Lloyd et al., 1987; Robertson et al., 1989). A second alternative is that ammonia is being consumed by bacteria. Van Duyl et al. (1993) suggested that short-term sedimentation events may stimulate bacterial growth which, in turn, may lead to a temporary immobilization of nitrogen in the increased bacterial biomass. A third alternative is that ammonia is oxidized directly to N_2 by the abundant authigenic manganese oxides in the sediment surface layer, thereby short-circuiting the nitrification-denitrification process altogether (Luther et al., 1997). Under the latter scenario, the overall reaction can be considered as the oxidation of ammonia to N_2 by oxygen, by using Mn (III,IV) as the catalyst. The stoichiometry of this reaction shows that the conversion of 1 mol ammonia to N_2 requires 3/4 mol O_2 :



This is less than half the oxygen requirement for the conversion of ammonia to nitrate, and would leave more oxygen available for other reactions. Finally, it has recently been demonstrated that ammonia can be oxidized by MnO_2 to nitrate as well (Hulth et al., 1999). Thus, there are several processes that can potentially intercept the ammonia flux from the sediment. Their relative importance remains to be worked out.

4.2.4. The reduction of manganese oxides within the anoxic sediment

In each of the three cores we observed a layer with high concentrations of nitrate deep within the anaerobic sediment. At St. 23B the nitrate concentration at 8 cm depth reached 50 μM . These concentrations are much higher than in the overlying bottom water, and we can therefore exclude the possibility that the high nitrate values are due to the infiltration of bottom water through animal burrows. It is conceivable that the nitrate maximum was caused by the oxidation of ammonia with oxygen, diffusing into the sediment through the walls of irrigated burrows (Aller, 1980), but the presence of high concentrations of Mn(II) at the same depth would argue against it. An interesting alternative, which does not require bioirrigation, is the oxidation of ammonia or organic-N by Mn(III) or Mn(IV). Hulth et al. (1999) have recently provided experimental evidence for anaerobic nitrate production through the oxidation of ammonia by MnO_2 , and Aller et al., (1998) invoked the following pathways to explain the persistence of NO_3^- at depth in Panama Basin sediments:



The coincidence of the nitrate maximum with the Mn(II) maximum observed in our cores is consistent with this mechanism.

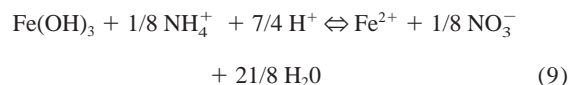
Hulth et al. (1999) estimated that Reaction 7 was energetically possible under typical sedimentary conditions. We can calculate the reaction quotients or ionic activity products (IAP) of Reactions 7: $(\text{Mn}^{2+})^{1/2}(\text{NO}_3^-)^{1/8}/(\text{H}^+)^{3/4}(\text{NH}_4^+)^{1/8}$, where (i) refer to activities, and 8: $(\text{Mn}^{2+})(\text{NO}_3^-)^{1/8}/(\text{H}^+)^{7/4}(\text{NH}_4^+)^{1/8}$ by using the measured pore-water concentrations at the depth of the subsurface nitrate maximum and estimates of the activity coefficients of Mn(II), NO_3^- , and NH_4^+ in seawater (Johnson, 1982; Klinkhammer, 1980; Millero and Pierrot, 1998). For St. 23, 23A, and 23B the calculated IAP(7) values are close to $10^{3.0}$ at pH 7 and $10^{3.7}$ at pH 8, and IAP(8) values are close to $10^{7.8}$ at pH 7 and $10^{9.5}$ at pH 8. These values are far below the equilibrium constant (K°) for Reactions 7 and 8, which are derived by using, respectively, pyrolusite ($\beta\text{-MnO}_2$, $K^\circ(7) = 10^{5.84}$) and manganite ($\gamma\text{-MnOOH}$, $K^\circ(8) = 10^{10.39}$) or feitknechtite ($\beta\text{-MnOOH}$, $K^\circ(8) = 10^{12.84}$) as possible Mn(IV and III) oxide minerals in St. Lawrence Estuary sediments (Hem and Lind, 1983). The large difference between K° values and IAPs means that NH_4^+ is metastable in the presence of manganese oxides whereas Mn(II) and NO_3^- can accumulate in pore

water at the concentration levels we measured and beyond. Therefore, the anaerobic production of nitrate through Reactions 7 or 8 is highly favored in the studied sediments whenever Mn(III,IV) enriched particles are biotransported into the anaerobic ammonia-rich zone.

4.3. The Role of Iron in the Diagenesis of Iodine and Nitrogen Species

4.3.1. Reactions involving Fe(III)

The sediment surface layer is also enriched in oxidized iron as inferred from the ascorbate leachable fraction. The oxidation of ammonia to N_2 by amorphous Fe(III) is only thermodynamically feasible at $\text{pH} < 6.8$ (Luther et al., 1997) and is therefore not likely to be involved in the removal of ammonia in the aerobic zone near the sediment-water interface. Oxidized iron can of course be transported downward into the anoxic sediment by advection and mixing but, as we will now show, the anaerobic oxidation of ammonia to nitrate by Fe(III) is unlikely. Applying the same reasoning as we did for manganese oxides above, ammonia would be oxidized by Fe(III) according to:



The equilibrium constant for this reaction, $K^\circ(9)$, is $10^{3.09}$ at 25°C by using ferrihydrite as Fe(III) phase. Reaction 9 only becomes favorable when $\text{IAP}(9) < K^\circ(9)$, i.e., when (Fe^{2+}) is below $10^{-10.7}$ at pH 8 or below 10^{-9} at pH 7. The activity coefficient for Fe^{2+} used here is that given by Millero (1982). Thus, nitrate production and accumulation in pore waters via Reaction 9 can only occur under conditions where dissolved Fe(II) remains at very low concentrations. In anaerobic non-sulfidic pore waters where Fe(II) is abundant, Reaction 9 is, therefore, less likely than Reactions 7 or 8.

4.3.2. Reactions involving Fe(II)

The upward flux of dissolved Fe(II) is intercepted at depths where nitrate is abundant and oxygen is absent. The oxidation of Fe(II) by nitrate is possible, and the reduction of nitrate to N_2 by Fe(II) is thermodynamically favorable at all pH (Luther et al., 1997). The oxidation of Fe(II) by nitrate has been observed to take place (Hansen et al., 1994; Postma, 1990) and the reaction can be mediated by nitrate-reducing bacteria (Straub et al., 1996). The most favorable product is green rust (Fe(II)-Fe(III) hydroxide-sulfate). Green rust can be oxidized further by nitrate to goethite (Hansen and Bender Koch, 1998). In our cores, the appearance of Fe(II) was accompanied by a broad peak at -0.4 V in the voltammogram, consistent with the presence of colloidal Fe(III) or dissolved Fe(III) complexes (Brendel, 1995; Huettel et al., 1998).

5. CONCLUSION

A multitude of redox reactions are possible during the early diagenesis of sediment, but their relative importance varies in time and space. For example, oxygen was not the major oxidant for the upward diffusing Mn(II) at the time our cores were

collected, yet the location of the solid-phase manganese peak near the oxic sediment–water interface points to oxygen as the ultimate oxidant for Mn(II). Vertical distributions of redox species in bioturbated sediments are often transient and not at steady state.

High-resolution profiles of redox species suggest the existence of reactions not usually considered in diagenetic studies. The many possibilities include the production of N_2 in reactions between ammonia and manganese oxides in the presence of oxygen, and between nitrate and iodide or Fe(II). These reactions would contribute to the observed high rates of N_2 production in continental margin sediments, complementing bacterial nitrification/denitrification. The possible reactions also include the anaerobic production of nitrate from ammonia and manganese oxides and the production of iodine via nitrate oxidation of iodide.

The high-resolution data show that iodine species can be quantitatively important in the diagenesis of manganese, despite the large concentration ratio between total Mn and total I in surface sediment. The data also show that significant removal of iodine is taking place below the iodide maximum. This is most likely due to the production of an oxidized iodine species, which in turn can react with the solid phase. Nitrate is an interesting candidate as the oxidant, because the reaction with I(-I) could yield N_2 and I_2 . This possibility is intriguing not only because it would promote denitrification, but also because I_2 is highly reactive and could react further with organic matter. This reaction would close the cycle whereby the iodine that is delivered to the sediment in association with organic matter is released to the pore water via hydrolysis, oxidized to a more reactive species, and finally recombined with organic matter and buried.

Many of the reactions and pathways discussed here need experimental confirmation and further field observation, but the important point is that a multitude of reactions are possible and that their relative importance will vary over time. The paradigm that the electron acceptor that yields the highest amount of free energy is used preferentially in the terminal step of the bacterially mediated oxidation of organic matter is not violated in bioturbated sediments, but the time sequence of redox reactions that follows from the paradigm does not always translate to a similarly recognizable depth sequence. Diagenesis in sediments affected by bioturbation and other physical disturbances should be thought of as a process that, through a mosaic of redox reactions, tends to but not always reaches a steady state.

Acknowledgments—Financial support from the Natural Science and Engineering Council of Canada to B.S. and A.M., and from the U.S. National Oceanic and Atmospheric Administration, Office of Sea Grant (NA16RG0162 to 03) to G.W.L. are gratefully acknowledged. We thank the editorial reviewers whose comments inspired us to improve our manuscript.

REFERENCES

- Aller R. C. (1980) Quantifying solute distributions in the bioturbated zone of marine sediments by defining an average microenvironment. *Geochim. Cosmochim. Acta* **44**, 1955–1965.
- Aller R. C. (1990) Bioturbation and manganese cycling in hemipelagic sediments. *Phil. Trans. R. Soc. Lond. A* **331**, 51–68.
- Aller R. C. (1994a) Bioturbation and remineralization of sedimentary organic matter: Effects of redox oscillation. *Chem. Geol.* **114**, 331–345.
- Aller R. C. (1994b) The sedimentary Mn cycle in Long Island Sound: Its role as intermediate oxidant and the influence of bioturbation, O_2 , and C_{org} flux on diagenetic reaction balances. *J. Mar. Res.* **52**, 259–295.
- Aller R. C., Hall P. O. J., Rude P. D., and Aller J. Y. (1998) Biogeochemical heterogeneity and suboxic diagenesis in hemipelagic sediments of the Panama Basin. *Deep-Sea Res. I* **45**, 133–165.
- Aller R. C. and Rude P. D. (1988) Complete oxidation of solid phase sulfides by manganese and bacteria in anoxic marine sediments. *Geochim. Cosmochim. Acta* **52**, 751–765.
- Anderson L. (1979) Simultaneous spectrophotometric determination of nitrite and nitrate by flow injection analysis. *Anal. Chim. Acta* **110**, 123–128.
- Anschutz P., Zhong S., Sundby B., Mucci A., and Gobeil C. (1998) Burial efficiency of phosphorus and the geochemistry of iron in continental margin sediments. *Limnol. Oceanogr.* **43**, 53–64.
- Arakaki T. and Morse J. W. (1993) Coprecipitation and adsorption of Mn^{2+} with mackinawite (FeS) under conditions similar to those found in anoxic sediments. *Geochim. Cosmochim. Acta* **57**, 1–15.
- Berner R. A. (1980) *Early Diagenesis. A Theoretical Approach*. Princeton Univ. Press.
- Boudreau B. P. (1996) The diffusive tortuosity of fine-grained un lithified sediments. *Geochim. Cosmochim. Acta* **60**, 3139–3142.
- Brendel P. J. (1995) Development of a mercury thin film voltammetric microelectrode for the determination of biogeochemically important redox species in porewaters of marine and freshwater sediments. Ph.D. Thesis, Univ. Delaware.
- Brendel P. J. and Luther G. W. III. (1995) Development of a gold amalgam voltammetric microelectrode for the determination of dissolved Fe, Mn, O_2 , and S(-II) in porewaters of marine and freshwater sediments. *Environ. Sci. Technol.* **29**, 751–761.
- Burdige D. J. and Gieskes J. M. (1983) A porewater/solid phase diagenetic model for manganese in marine sediments. *Am. J. Sci.* **283**, 29–47.
- Edenborn H. M., Mucci A., Silverberg N., and Sundby B. (1987) Sulfate reduction in deep coastal marine sediments. *Mar. Chem.* **21**, 329–345.
- Ferdelman T. G. (1988) The distribution of sulfur, iron, manganese, copper and uranium in salt marsh sediment cores as determined by sequential extraction methods. M.Sc. Thesis, Univ. Delaware.
- François R. (1987) The influence of humic substances on the geochemistry of iodine in nearshore and hemipelagic marine sediments. *Geochim. Cosmochim. Acta* **51**, 2417–2427.
- Frette L., Gejlsbjerg B., and Westermann P. (1997) Aerobic denitrifiers isolated from an alternating activated sludge system. *FEMS Microbiol. Ecol.* **24**, 363–370.
- Froelich P. N., Klinkhammer G. P., Bender M. L., Luedtke N. A., Heath G. R., Cullen D., Dauphin P., Hammond D., Hartman B., and Maynard V. (1979) Early oxidation of organic matter in pelagic sediments of the eastern equatorial Atlantic: Suboxic diagenesis. *Geochim. Cosmochim. Acta* **43**, 1075–1090.
- Gagnon C., Mucci A., and Pelletier E. (1995) Anomalous accumulation of acid-volatile sulphides (AVS) in a coastal marine sediment, Saguenay Fjord, Canada. *Geochim. Cosmochim. Acta* **59**, 2663–2675.
- Gobeil C., Macdonald R. W., and Sundby B. (1997) Diagenetic separation of cadmium and manganese in suboxic continental margin sediments. *Geochim. Cosmochim. Acta* **61**, 4647–4645.
- Hall P. O. J. and Aller R. C. (1992) Rapid, small-volume flow injection analysis for ΣCO_2 and NH_4^+ in marine and freshwaters. *Limnol. Oceanogr.* **37**, 1113–1119.
- Hall P., Anderson L., Rutgers van der Loeff M., Sundby B., and Westerlund S. (1989) Oxygen uptake kinetics at the sediment–water interface. *Limnol. Oceanogr.* **34**, 734–746.
- Hansen H. C. B. and Bender Koch C. (1998) Reduction of nitrate to ammonium by suphate green rust: Activation energy and reaction mechanism. *Clay Miner.* **33**, 87–101.
- Hansen H. C. B., Borggaard O. K., and Sorensen J. (1994) Evaluation of the free energy of formation of Fe(II)–Fe(III) hydroxide–sulphate (green rust) and its reduction of nitrite. *Geochim. Cosmochim. Acta* **58**, 2599–2608.
- Hem J. D., and Lind C. J. (1983) Nonequilibrium models for predicting

- forms of precipitated manganese oxides. *Geochim. Cosmochim. Acta* **47**, 2037–2046.
- Huerta-Díaz M. A. and Morse J. W. (1990) A quantitative method for determination of trace metal concentrations in sedimentary pyrite. *Mar. Chem.* **29**, 119–144.
- Huerta-Díaz M. A. and Morse J. W. (1992) Pyritization of trace metals in anoxic marine sediments. *Geochim. Cosmochim. Acta* **56**, 2681–2702.
- Huettel M., Ziebis W., Forster S., and Luther G. W. III (1998) Advective transport affecting metal and nutrient distributions and interfacial fluxes in permeable sediments. *Geochim. Cosmochim. Acta* **62**, 613–631.
- Hulth S., Blackburn T. H., and Hall P. O. J. (1994) Arctic sediments (Svalbard): consumption and microdistribution of oxygen. *Mar. Chem.* **46**, 293–316.
- Hulth S., Aller R. C., and Gilbert F. (1999) Coupled anoxic nitrification/manganese reduction in marine sediments. *Geochim. Cosmochim. Acta* **63**, 49–66.
- Johnson K. S. (1982) Solubility of rhodochrosite (MnCO₃) in water and seawater. *Geochim. Cosmochim. Acta* **46**, 1805–1809.
- Kennedy H. A. and Elderfield H. (1987) Iodine diagenesis in pelagic deep-sea sediments. *Geochim. Cosmochim. Acta* **51**, 2489–2504.
- Klinkhammer G. P. (1980) Early diagenesis in sediments from the eastern equatorial Pacific. II. Pore water metal results. *Earth Planet. Sci. Lett.* **7**, 265–270.
- Kostka J. E. and Luther G. W. III (1994) Partitioning and speciation of solid phase iron in saltmarsh sediments. *Geochim. Cosmochim. Acta* **58**, 1701–1710.
- Li Y. H. and Gregory S. (1974) Diffusion of ions in sea water and in deep-sea sediments. *Geochim. Cosmochim. Acta* **38**, 703–714.
- Lloyd D., Boddy L., and Davies K. J. P. (1987) Persistence of bacterial denitrification capacity under aerobic conditions: The rule rather than the exception. *FEMS Microbiol. Ecol.* **45**, 185–190.
- Luther G. W. III, Branson Swartz C., and Ullman W. J. (1988) Direct determination of iodide in seawater by cathodic stripping square wave voltametry. *Anal. Chem.* **60**, 1721–1724.
- Luther G. W. III, Brendel P. J., Lewis B. L., Sundby B., Lefrançois L., Silverberg N., and Nuzzio D. (1998) Oxygen, manganese, iron, iodide, and sulfide distributions in pore waters of marine sediments measured simultaneously with a solid state voltammetric microelectrode. *Limnol. Oceanogr.* **43**, 325–333.
- Luther G. W. III, Sundby B., Lewis G. L., Brendel P. J., and Silverberg N. (1997) Interactions of manganese with the nitrogen cycle: Alternative pathways for dinitrogen formation. *Geochim. Cosmochim. Acta* **61**, 4043–4052.
- Luther G. W. III, Reimers C. E., Nuzzio D. B., and Lovalvo D. (1999) In situ deployment of voltammetric, potentiometric, and amperometric microelectrodes from ROV to determine dissolved O₂, Mn, Fe, S(–2), and pH in porewaters. *Environ. Sci. Technol.* **33**, 4352–4356.
- Middelburg J. J., De Lange G. J., and Van der Weijden C. H. (1987) Manganese solubility control in marine pore waters. *Geochim. Cosmochim. Acta* **51**, 759–763.
- Millero F. J. (1982) Use of models to determine ionic interactions in natural waters. *Thalassia Jugoslavia* **18**, 253–291.
- Millero F. J. and Pierrot D. (1998) A chemical equilibrium model for natural waters. *Aquatic Geochem* **4**, 153–199.
- Mucci A. (submitted) The solubility of pseudokutnahorite, Mn-Ca(CO₃)₂, in water and seawater: Control of manganese concentration in marine porewaters. *Geochim. Cosmochim. Acta*.
- Murray J. W., Codispoti L. A., and Friederich G. E. (1995) Oxidation–reduction environments: The suboxic zone of the Black Sea. In *Aquatic Chemistry: Interfacial and Interspecies Processes* (ed. C. P. Huang et al.), Vol. 244, pp. 157–176. Am. Chem. Soc.
- Postma D. (1990) Kinetics of nitrate reduction by detrital Fe(II)-silicates. *Geochim. Cosmochim. Acta* **54**, 903–908.
- Postma D. and Jakobsen R. (1996) Redox zonation: Equilibrium con-
- strains on the Fe(III)/SO₄-reduction interface. *Geochim. Cosmochim. Acta* **60**, 3169–3175.
- Raiswell R., Canfield D. E., and Berner R. A. (1994) A comparison of iron extraction methods for the determination of degree of pyritisation and the recognition of iron-limited pyrite formation. *Chem. Geol.* **111**, 101–110.
- Rapin F., Tessier A., Campbell P. G. C., and Richard R. (1986) Potential artifacts in the determination of metal partitioning in sediments by a sequential extraction procedure. *Environ. Sci. Technol.* **20**, 836–840.
- Robertson L. A., Cornelisse R., de Vos P., Hadioetomo R., and Kuenen J. G. (1989) Aerobic denitrification in various heterotrophic nitrifiers. *Antonie van Leeuwenhoek* **56**, 289–299.
- Schulz H. D., Dahmke A., Schnizel U., Wallmann K., and Zabel M. (1994) Early diagenetic processes, fluxes, and reaction rates in sediments of the South Atlantic. *Geochim. Cosmochim. Acta* **58**, 2041–2060.
- Shimmield G. B. and Pedersen T. F. (1990) The geochemistry of reactive trace metals and halogens in hemipelagic continental margin sediments. *Aquat. Sci.* **3**, 255–279.
- Silverberg N., Bakker J., Edenborn H., and Sundby B. (1987) Oxygen profiles and organic carbon fluxes in Laurentian Trough sediments. *Neth. J. Sea Res.* **21**, 95–105.
- Silverberg N., Nguyen H. V., Delibrias G., Koide M., Sundby B., Yokoyama Y., and Chesselet R. (1986) Radionuclide profiles, sedimentation rates, and bioturbation in modern sediments of the Laurentian Trough, Gulf of St. Lawrence. *Oceanol. Acta* **9**, 285–290.
- Silverberg N. and Sundby B. (1990) Early diagenesis and sediment–water interaction in the Laurentian Trough. In *Oceanography of a Large-Scale Estuarine System: The St. Lawrence* (eds. M. I. El-Sabh and N. Silverberg), Vol. 39, pp. 202–238. Springer-Verlag.
- Sørensen J., Jørgensen K. S., Colley S., Hydes D. J., Thomson J., and Wilson T. R. S. (1987) Depth localization of denitrification in a deep-sea sediment from the Madeira Abyssal Plain. *Limnol. Oceanogr.* **32**, 758–762.
- Straub K. L., Benz M., Schink B., and Widdel F. (1996) Anaerobic, nitrate-dependant microbial oxidation of ferrous iron. *Appl. Environ. Microbiol.* **62**, 1458–1460.
- Stumm W. and Morgan J. J. (1996) *Aquatic Chemistry*, 3rd ed. John Wiley & Sons.
- Sundby B., Silverberg N., and Chesselet R. (1981) Pathways of manganese in an open estuarine system. *Geochim. Cosmochim. Acta* **45**, 293–307.
- Taillefert M., Bono A., and Luther G. W. III (2000) Reactivity of freshly formed Fe(III) in synthetic solutions and porewaters: Voltammetric evidence of an aging process. *Environ. Sci. Technol.* (in press).
- Takayanagi K. and Cossa D. (1985) Behaviour of dissolved iodine in the upper St. Lawrence Estuary. *Can. J. Earth Sci.* **22**, 644–646.
- Truesdale V. W. (1982) The fate of molecular iodine added to sea water. *Mar. Chem.* **11**, 87.
- Ullman W. J. and Aller R. C. (1983) Rates of iodine remineralization in terrigenous near-shore sediments. *Geochim. Cosmochim. Acta* **47**, 1423–1432.
- Ullman W. J. and Aller R. C. (1985) The geochemistry of iodine in near-shore carbonate sediments. *Geochim. Cosmochim. Acta* **49**, 967–978.
- Ullman W. J. and Sandstrom M. W. (1987) Dissolved nutrient fluxes from the nearshore sediments of Bowling Green Bay, Central Great Barrier Reef Lagoon (Australia). *Estuar. Coast. Shelf Sci.* **24**, 289–303.
- Van Duyl F. C., Van Raaphorst W., and Kop A. J. (1993) Benthic bacterial production and nutrient sediment–water exchange in sandy North Sea sediments. *Mar. Ecol. Progr. Ser.* **100**, 85–95.
- Yeats P. A. (1988) Nutrients. In *Chem. Oceanography in the Gulf of St. Lawrence* (ed. P. M. Strain), *Can. Bull. Fish. Aquat. Sci.* **220**, 1.